

# PROGRESS IN UNDERSTANDING BLAZARS FROM *BeppoSAX* OBSERVATIONS

L. Maraschi<sup>1</sup>, L. Chiappetti<sup>2</sup>, G. Fossati<sup>3</sup>, E. Pian<sup>4</sup> and F. Tavecchio<sup>1</sup>

<sup>1</sup>*Astronomical Observatory of Brera, via Brera 28, 20121 Milano, Italy*

<sup>2</sup>*IFCTR, CNR, via Bassini 15, 20133 Milano, Italy*

<sup>3</sup>*SISSA/ISAS, Via Beirut 2-4, I-34014 Miramare (Trieste), Italy*

<sup>4</sup>*ITESRE, C.N.R., Via Gobetti 101, I-40129 Bologna, Italy*

## ABSTRACT

Results obtained with *BeppoSAX* observations of blazars within various collaborative programs are presented. The spectral similarity “paradigm”, whereby the spectral energy distributions of blazars follow a sequence, leading to a unified view of the whole population, is briefly illustrated. We concentrate on recent observations of flares and associated spectral variability long for three objects at the “blue” end of the spectral sequence, namely PKS 2155–304, Mkn 421 and Mkn 501. The results are discussed in terms of a general analytic synchrotron self-Compton interpretation of the overall spectrum. The physical parameters of the quasi-stationary emission region can be derived with some confidence, while the variability mechanism(s) must be complex.

## 1 INTRODUCTION

One of the most poorly understood phenomena in AGN is the origin of relativistic jets. Their existence, previously inferred from indirect arguments (Blandford & Rees 1978), was spectacularly demonstrated by the observation of superluminal expansion of the knots in the radio jets on the parsec scale. The unified scheme of AGN postulates that all radio-loud AGN possess relativistic jets and that blazars are the subset where the jet happens to point at a small angle to the line of sight. Because the plasma flows in the jet at relativistic speed the emitted radiation is concentrated in a narrow cone (beam) along the direction of motion. An observer at small angle to the beam will receive radiation strongly enhanced by Doppler boosting.

In blazars the non thermal continuum received from the jet is largely dominant over the more isotropic radiation emitted by the surrounding gas or stars. Therefore they are the best laboratory to probe the processes at work in relativistic jets. Understanding the radiation mechanisms allows reconstructing the spectra of relativistic particles and discussing the mechanisms of particle acceleration and energy transport along the jet and ultimately their origin.

## 2 THE SPECTRAL ENERGY DISTRIBUTIONS OF BLAZARS

Observationally, blazars are characterised by a strong radio core with flat or inverted spectrum, and by an extremely luminous broad band continuum, highly variable at all wavelengths. After the launch of the

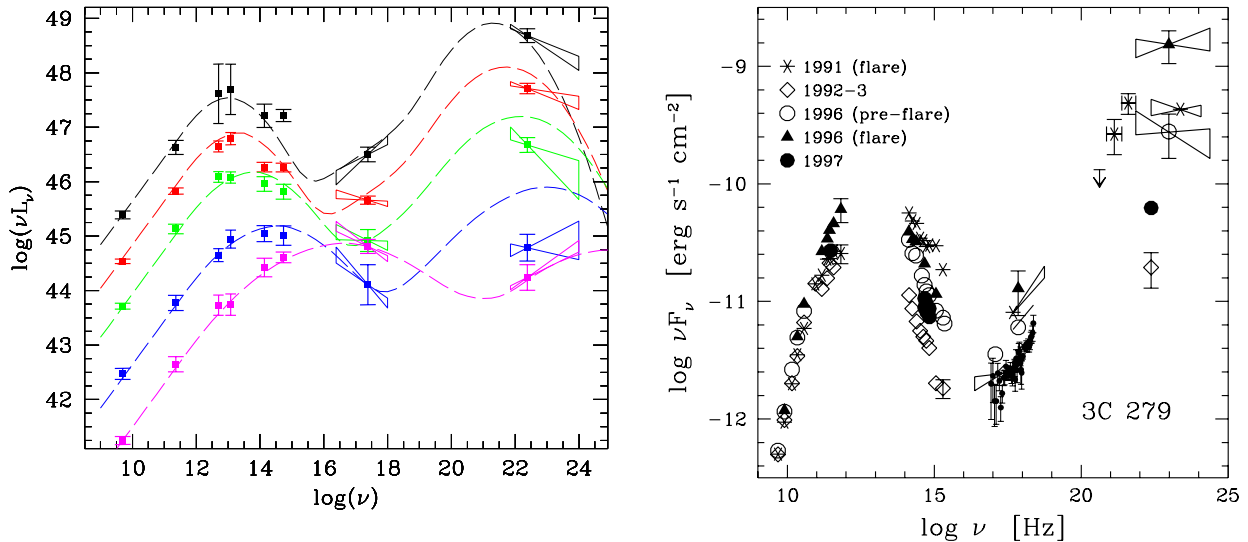


Figure 1: *Left panel:* Average SEDs of the “merged” blazar sample binned according to radio luminosity, irrespective of the original classification. Empty asymmetric triangles represent uncertainties in spectral shapes as measured in the X-ray and  $\gamma$ -ray bands. The overlaid dashed curves are analytic approximations obtained assuming that the ratio of the two peak frequencies is constant and that the luminosity of the second peak is proportional to the radio luminosity (from Fossati et al. 1998). *Right panel:* Radio-to- $\gamma$ -ray energy distribution of 3C 279 at different epochs. The X-ray spectrum observed with *BeppoSAX* on January 1997 is shown, together with the simultaneously measured optical and  $\gamma$ -ray fluxes. Data obtained in June 1991, and December 1992-January 1993 are from Maraschi et al. (1994). The pre-flare and flaring state data in January-February 1996 are from Wehrle et al. (1998). The UV, optical and near-IR data have been corrected for Galactic extinction.

CGRO it was discovered that this continuum extends into the  $\gamma$ -ray range and most importantly that the  $\gamma$ -ray luminosity represents a large fraction of the total emitted power.

The presence or absence of broad emission lines in the optical-UV spectrum has led to distinguish quasar-like objects from BL Lac type objects. However there are arguments to believe that these differences, rather than representing a genuine dichotomy in the type of processes occurring at the nucleus may arise from different physical conditions outside the jet (e.g., Bicknell 1994). Support to this unifying view comes from a comparison of the overall spectral shapes of different subclasses of blazars.

To this end we collected multiwavelength data for three complete samples of blazars, the 2 Jy sample of flat spectrum radio-loud quasars (FSRQ) the 1 Jy sample of BL Lac objects and the X-ray selected BL Lacs from the Einstein Slew Survey (see Fossati et al. 1998 for full information and references). The results are shown in Fig. 1, where the three samples have been merged and the total sample has been binned according to radio-luminosity only. From the figure it is apparent that:

- All the spectral energy distributions (SED) in the  $\nu f_\nu$  representation are characterized by two peaks, indicating two main spectral components.
- The first peak falls at lower frequency for higher luminosity objects
- The second peak frequency seems to correlate with the first one, as indicated by the  $\gamma$ -ray and X-ray slopes. The curves drawn as reference correspond to a fixed ratio between the two peak frequencies.

Although one should be aware that selection biases may affect the results (see Fossati et al. 1997), Figure 1 suggests that the SEDs of all blazars are globally similar and lie along a continuous spectral

sequence. For the most luminous objects the first peak falls at frequencies lower than the optical band, while for the least luminous ones the reverse is true. Thus highly luminous objects have steep (“red”) optical-UV continua, while low luminosity objects with peak frequency beyond the UV range have flat (“blue”) optical-UV continua. For brevity we will refer to objects on the high and low luminosity end of the sequence as “red” or “blue” blazars.

### 3 IMPORTANCE OF MULTIWAVELENGTH VARIABILITY

It is generally thought that the first spectral component is due to synchrotron radiation. The spectra from the radio to the submillimeter range most likely involve superposed contributions from different regions of the jet with different self-absorption turnovers. From infrared (IR) frequencies upwards the synchrotron emission should be thin and could be produced in a single zone of the jet, allowing adoption of a homogeneous model.

The second spectral component (peaking in  $\gamma$ -rays) could be produced by the high energy electrons responsible for the synchrotron component, upscattering soft photons via the inverse Compton process (IC). (e.g., Sikora 1994; Ulrich, Maraschi, & Urry, 1997 (UMU97), and references therein).

An immediate consequence of this interpretation is that changes in the electron population should produce correlated variability in the two components. Different models for the soft photon source(s) (the synchrotron photons themselves, synchrotron self-Compton, SSC; photons from a possible accretion disk, or related broad line region, EC; synchrotron photons backscattered from gas clouds close to the jet, “mirror Compton”, MC, see e.g., UMU97, and references therein) imply different possible ways of variability of the IC component. For instance in the SSC model the Compton component must vary with the synchrotron component and with larger amplitude (in the Thomson regime), while in the EC model variations of the IC component without associated variations in the synchrotron component should be possible (Ghisellini & Maraschi 1996). However in the case MC model variability could closely mimic the SSC type. Clearly the study of correlated variability at frequencies close to the two peaks of the SED is an essential tool to constrain models.

It is important to stress that in blue blazars the X-ray range represents the high energy end of the synchrotron component. Deriving from extremely energetic electrons, with short lifetimes the X-ray emission from blue blazars is rapidly variable. The associated IC emission falls beyond the EGRET energy range and is detectable in the TeV band for the few brightest objects. This offers the possibility of ground based monitoring at the highest energies (VHE) and makes the study of the X-ray/TeV correlation extremely interesting.

For red blazars the corresponding energy ranges are from the IR to the UV (1-10 eV) for the synchrotron component and from the MeV to the GeV bands for the IC component, while X-rays represent the low energy end of the IC component. Correlation studies of the IR to UV emission on one hand with the X-ray to  $\gamma$ -ray emission on the other have been performed by several groups (see UMU97 and refs therein). The most intensively observed object has been 3C 279. Repeated intensive multiwavelength campaigns have detected a series of high and low states with rather regular spectral variations. The synchrotron intensity is indeed correlated with the IC intensity at least on long time scales with  $\gamma$ -rays showing the largest variability amplitude. The *BeppoSAX* data obtained in 1997, when the source was in an intermediate intensity state, confirm this trend (see Fig. 1, from Maraschi 1998).

Unfortunately, the exhaustion of gas is causing substantial degradation of the EGRET sensitivity, practically preventing further monitoring in  $\gamma$ -rays. At the same time the developing capabilities of the ground based Cherenkov telescopes allow improved monitoring at TeV energies, shifting the focus of multiwavelength studies from red to blue blazars.

Therefore we will concentrate here on *BeppoSAX* results concerning three bright blue blazars detected in the TeV band, PKS 2155–304, Mkn 501 and Mkn 421. Other important results obtained with *BeppoSAX* concern the spectral variability of the third blue BL Lac detected at TeV energies (Giommi et al. 1998a), the X-ray spectra of bright, red blazars (e.g., Ghisellini et al. 1998) and of other BL Lac samples (e.g., Wolter et al. 1998, Padovani et al. 1998).

## 4 PKS 2155–304

PKS 2155–304 is one of the brightest BL Lacertae objects in the X-ray band and one of the few detected in  $\gamma$ -rays by the EGRET experiment on CGRO (Vestrand et al. 1995). It was observed by *BeppoSAX* during the PV phase (Giommi et al. 1998b). No observations at other wavelengths simultaneous with the  $\gamma$ -ray ones were ever obtained for this source, yet it is essential to measure the IC and synchrotron peaks at the same time in order to constrain emission models unambiguously (e.g., Dermer et al. 1997, Tavecchio, Maraschi, & Ghisellini 1998). For these reasons, having been informed by the EGRET team of their observing plan and of the positive results of the first days of the CGRO observation, we asked to swap a prescheduled target of our *BeppoSAX* blazar program with PKS 2155–304. In 1997 November 11-17 (Sreekumar & Vestrand 1997) the  $\gamma$ -ray flux from PKS 2155–304 was very high, roughly a factor of three greater than the previously published value from this object. *BeppoSAX* pointed PKS 2155–304 for about 1.5 days starting on November 22. Quick-look analysis indicated that also the X-ray flux was close to the highest recorded levels (Chiappetti & Torroni 1997). A paper on these data is currently submitted for publication (Chiappetti et al. 1998). Here we summarise the most important results.

### i) *Light Curves*

Fig. 2 (left panel) shows the light curves binned over 1000 sec obtained in different energy bands, 0.1-1.5 keV (LECS) and 3.5-10 keV (MECS). The light curves show a clear high amplitude variability: three peaks can be identified. The most rapid variation observed (the decline from the peak at the start of the observation) has a halving timescale of about  $2 \times 10^4$  s, similar to previous occasions (see e.g., Urry et al. 1997). No shorter time scale variability is detected although our observations would have been sensitive to doubling timescales of order  $10^3$  s. The variability amplitude is energy dependent being larger at higher energies. The hardness ratio correlates positively with the flux, indicating that states with higher flux have harder spectra.

We looked for time lags between variations at different energies as suggested by previous ASCA observations of the same source and of Mkn 421 (Makino this volume; Takahashi et al. 1996). The possible presence of a soft lag is indicated by the fact that the maximum hardness ratio occurs *before* maximum intensity. Using the Discrete Correlation Function (Edelson & Krolik 1988) and fitting its maximum with a Gaussian we estimate from its peak a lag of  $0.49 \pm 0.08$  ( $1-\sigma$ ). A more detailed discussion of the issue of lags in this source, including comparison with previous observations and error estimates through Monte Carlo simulations is given in Treves et al. (1998).

### ii) *Spectra*

We found that the *joint* LECS and MECS spectra could not be adequately fitted by either a single or a broken power law (bpl). A single power law is unacceptable even in each spectral range while a bpl model with Galactic absorption yields good fits to the data of each instrument with consistent slopes at the high energy end of the LECS and at the low energy end of the MECS. We therefore adopted this model as an approximation to a more realistic continuously curved spectral shape (see Giommi et al. 1998b) The spectral indices derived from separate bpl fits to the LECS and MECS data integrated over the whole observation are reported in Table 1, which allows comparison with the other two sources discussed below. The change in slope between the softest (0.1-1 keV) and hardest (3-10 keV) energy ranges is  $\simeq 0.8$ .

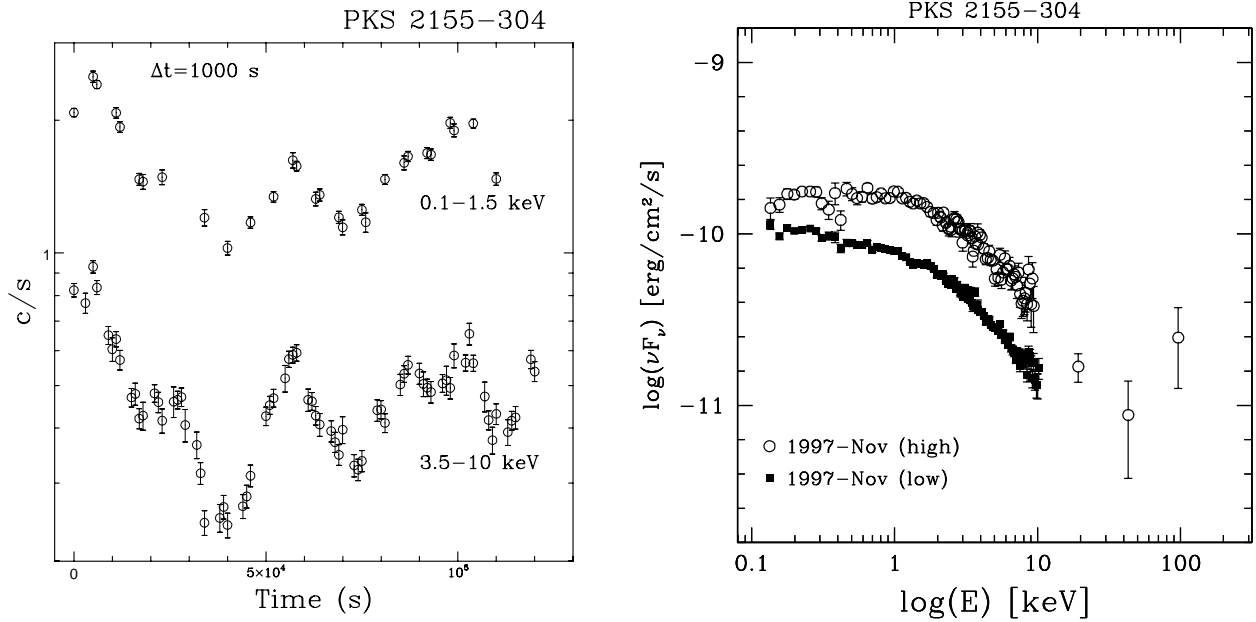


Figure 2: *Left panel:* Soft (0.1–1.5 keV) and medium (3.5–10 keV) light curves (in logarithmic scale) obtained from the November 1997 observation of PKS 2155–304 with *BeppoSAX*. *Right panel:* Deconvolved X-ray spectra of PKS 2155–304 in the highest and lowest states observed in November 1997. The open circles between 10 and 100 keV represent the PDS data, which are averages over the whole observation.

Fitting together the MECS and PDS data yields spectral parameters very similar to those obtained for the MECS alone. The residuals show that the PDS data are consistent with an extrapolation of the MECS fits up to about 50 keV. Above this energy the PDS data show an excess indicating a flattening of the spectrum.

The spectrum at the flare peak is harder than at lower intensity, as can be seen by computing directly the ratio of the count rate spectra as a function of energy, yet the spectral change is small and for bpl fits of the separate instruments the derived parameters are only marginally different. The deconvolved spectra are shown in Fig. 2 (right panel).

## 5 Mkn 421

Mkn 421, closely similar to PKS 2155–304 in brightness and spectral shape at UV and X-ray wavelengths was observed by *BeppoSAX* in April 1998 as part of a large multiwavelength campaign based on a week of continuous observation with ASCA and simultaneous monitoring with the available Cherenkov telescopes, Whipple, HEGRA and CAT. The *BeppoSAX* observations were scheduled before the ASCA ones in order to extend the coverage in time. A well defined pronounced flare was observed at the beginning of the observation reaching the peak in about 3 hrs and decaying in half a day. Due to its bright state the source was well visible also in the high energy instrument, the PDS.

### i) Light Curves

The light curves in three energy bands, derived from the LECS, MECS and PDS, all normalised to their respective average intensity, are shown in Fig. 3. The amplitude of variability increases and the decay time scales decrease with increasing energy although the latter effect is difficult to quantify without a specific model for the light curve.

It is interesting to explore whether the light curves at different frequencies show lags as observed previously

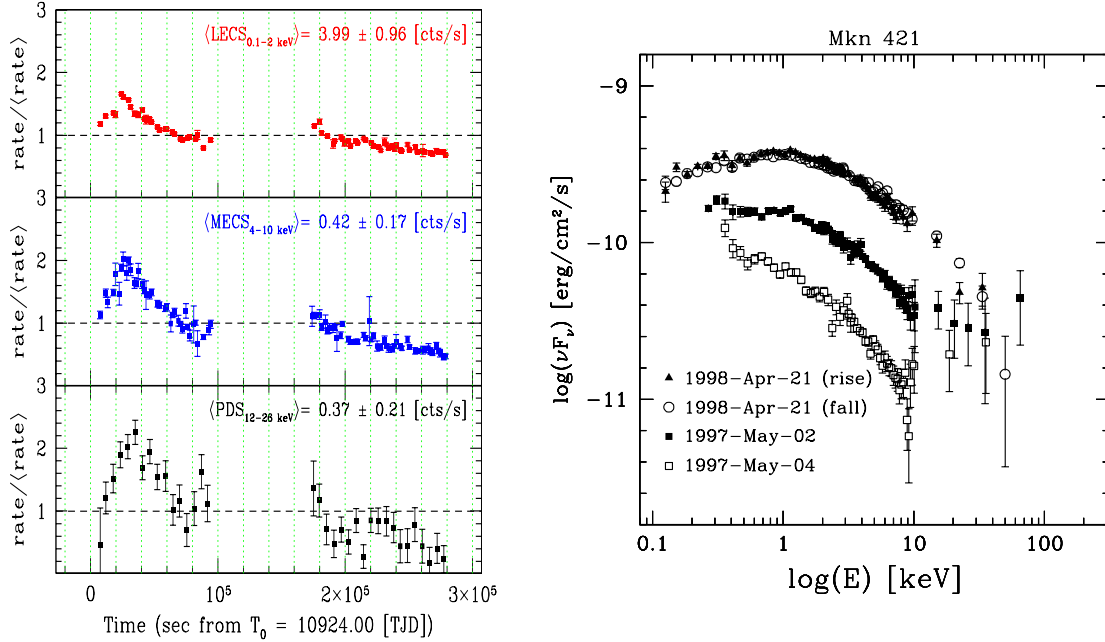


Figure 3: *Left panel*: light curves of Mkn 421 observed in April 21-24 in the 0.1-2 keV (LECS), 4-10 keV (MECS) and 12-26 keV (PDS) energy bands (top to bottom). Average count rates in each band with their dispersions are given. *Right panel*: Deconvolved X-ray spectra obtained with *BeppoSAX* in 1998 and 1997.

in this source by Takahashi et al. (1996). A first analysis with the DCF method reveals that, contrary to the case of PKS 2155–304 and of the 1994 flare of Mkn 421, in the present flare the soft photons *lead* the medium energy ones by about 1500 sec. The significance of this result needs to be assessed by a reliable estimate of the errors of the DCF method, however we can definitely exclude that lags or leads larger than this value are present.

## ii) Spectra

The shape of the X-ray spectra is qualitatively similar to the case of PKS 2155–304 and similar considerations apply. The spectral indices derived from separate bpl fits to the LECS and MECS data for 1998 April 21, which cover the whole flare, and for 1997 May 4 are reported in Table 1. The change in slope between the softest (0.1-1 keV) and hardest (3-10 keV) energy ranges is  $\simeq 0.8$  in both cases. Deconvolved spectra are compared in Fig. 3. It is apparent that the peak in the power distribution moves to higher energies with increasing intensity, reaching 1 keV during the flare.

## 6 Mkn 501

*BeppoSAX* observations of Mkn 501 in April 1997 revealed a completely new behavior. The spectra showed that at that epoch the synchrotron component peaked at 100 keV or higher energies, implying a shift of at least two orders of magnitude of the peak energy with respect to the quiescent state (Pian et al. 1998). Correspondingly the source was extremely bright in the TeV band and exhibited rapid flares (Catanese et al. 1997, Aharonian et al. 1997). The source was reobserved with *BeppoSAX* at three epochs, on 28, 29 April and 1 May 1998, for  $\sim 10$  hours, simultaneously with ground-based optical and TeV Cherenkov telescopes (Whipple and HEGRA).

For all epochs, fits to all the data either with a single or a broken power-law are unacceptable. The “curvature” in the LECS-MECS range is however smaller than for the previous two sources and a bpl fit to the joint LECS-MECS spectra gives a satisfactory result. The joint MECS, HPGSPC and PDS

Table 1: Comparison of spectral parameters of different sources

Epoch	$\alpha_1$	$E_{break,1}$ keV	$\alpha_2$	$E_{break,2}$ keV	$\alpha_3$
Mkn 501–97 April 17 <sup>a</sup>	$0.40^{+0.02}_{-0.04}$	$2.14^{+0.3}_{-0.5}$	$0.59^{+0.02}_{-0.01}$	$\sim 20$	$0.84 \pm 0.04$
Mkn 501–98 April 29	$0.48 \pm 0.04$	$1.3 \pm 0.4$	$0.83 \pm 0.05$	$17 \pm 5$	$1.15 \pm 0.05$
Mkn 501–98 May 01	$0.62 \pm 0.04$	$1.9 \pm 0.4$	$1.00 \pm 0.05$	$23 \pm 5$	$1.45 \pm 0.05$
Mkn 421–97 April 21 <sup>b</sup>	$0.85 \pm 0.03$	$1.13 \pm 0.11$	$1.40 \pm 0.1$	$3.73 \pm 1.00$	$1.68^{+0.12}_{-0.09}$
Mkn 421–98 May 4	$1.30 \pm 0.03$	$1.13 \pm 0.16$	$1.67 \pm 0.4$	$2.93 \pm 0.56$	$2.15 \pm 0.1$
PKS 2155–97 Nov <sup>b</sup>	$1.06 \pm 0.02$	$1.09 \pm 0.07$	$1.59 \pm 0.1$	$3.24 \pm 1.00$	$1.88^{+0.07}_{-0.03}$

<sup>a</sup>  $\alpha_1$  and  $\alpha_2$  are obtained from broken power law fits of the LECS+MECS data;

$\alpha_3$  is obtained from broken power law fits to MECS+PDS data.

<sup>b</sup>  $\alpha_1$  is obtained fitting LECS data with a broken power law,  $\alpha_3$  is obtained from broken power law fits to MECS data, while  $\alpha_2$  is the average of the spectral indices obtained from the previous fits in the common energy range of LECS and MECS data.

spectra are also well fitted with a bpl model. The spectral indices, obtained by fixing the value of the hydrogen column density to the Galactic value ( $1.73 \times 10^{20} \text{ cm}^{-2}$ , from Lockman & Savage 1995), are reported in Table 1. The deconvolved spectra of 1998 are compared in Fig. 4 (right panel) with that of the 1997 flare.

The 2-10 keV flux observed from Mkn 501 in April-May 1998 was close to that measured on 7 April 1997, namely the lowest observed with *BeppoSAX*, but substantially higher than observed historically. In 1998 the synchrotron peak was located at an energy of  $\sim 20$  keV, much lower than on April 97, but still exceptionally high compared to the two sources discussed above and even to most blue blazars, except possibly for 1ES2344+514 (Giommi et al. 1998). As in the cases shown above, the synchrotron peak is at higher energies during brighter states and in a given energy range the spectra flatten with increasing intensity. However spectral variations are small at energies much below the peak.

The TeV flux measured in April-May 1998 by the Whipple and HEGRA telescopes was definitely lower than observed last year at the beginning of the simultaneous X-ray and TeV outburst. Since the X-ray spectra at the two epochs differed mainly in the 20-100 keV band, we are led to conclude that the TeV emission is most likely produced through IC scattering off the high energy electrons which radiate in the hard X-ray band via the synchrotron mechanism. If this hypothesis is correct, then, analogously to the synchrotron radiation peak, also the IC peak must have shifted toward lower energies causing significant spectral changes in the TeV band.

## 7 PRESENT UNDERSTANDING AND OPEN PROBLEMS

The simplest model one can consider, applicable to all the sources discussed above, attributes the high energy radiation to SSC emission from a homogeneous spherical region of radius  $R$ , whose motion can be characterized by a Doppler factor  $\delta$ , pervaded by a magnetic field  $B$  and filled with relativistic particles with energy distribution described by a bpl (the latter corresponds to 4 parameters: two indices  $n_1, n_2$ , a break Lorentz factor  $\gamma_b$  and a normalization constant).

This seven parameter model is strongly constrained if observations provide a determination of the two slopes (in the X- and  $\gamma$ -ray bands), the frequency and flux of the synchrotron peak, the frequency and flux of the IC peak. Assuming  $R = ct_{var}$  the system is practically closed. We refer to Tavecchio, Maraschi

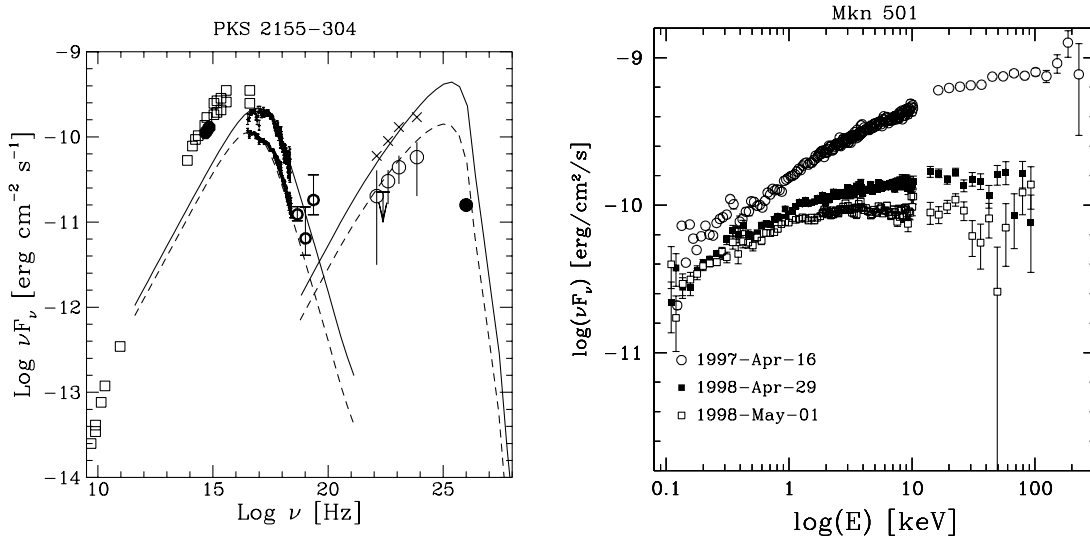


Figure 4: *Left panel:* SED of PKS 2155–304 compared with computed SSC models. X-ray data points are from the high and low intensity states measured by *BeppoSAX* in November 1997. The data at lower frequencies are from previous non simultaneous observations. Open circles represent the  $\gamma$ -ray data of 1995 and crosses the bright  $\gamma$ -ray state which triggered the *BeppoSAX* observations (from Maraschi et al. 1998). The filled circle represents the TeV flux recently announced by Chadwick et al. (1998). The values of the parameters used in the model computations are:  $\delta = 18$ ,  $B=1$  G,  $K = 10^{4.68}$ ,  $R = 3 \cdot 10^{15}$  cm,  $\gamma_b = 10^{4.49}$ ,  $n_1 = 2$ ,  $n_2 = 4.85$  (low state) and  $\delta = 18$ ,  $B=1$  G,  $K = 10^{4.8}$ ,  $R = 3 \cdot 10^{15}$  cm,  $\gamma_b = 10^{4.65}$ ,  $n_1 = 2$ ,  $n_2 = 4.85$  (high state). *Right panel:* Deconvolved X-ray spectra of Mkn 501 obtained from *BeppoSAX* during 1997 April 16 (open circles), 1998 April 29 (filled squares) and 1998 May 1 (open squares).

& Ghisellini (1998) for a general analytic procedure to determine the physical parameters of different sources in this class of models. The main point we wish to stress is that there is little uncertainty on the model parameters if both peaks can be measured simultaneously, and even when some of the values (e.g., the peak energy of the IC component) are lacking, the shape of the SED constrains the parameters in relatively restricted ranges. In fact, different authors find closely similar parameters even when using somewhat different formulations of the SSC model (e.g., Mastichiadis & Kirk 1997, Ghisellini, Maraschi, Dondi 1996 for Mkn 421).

As an illustration, we show in Fig. 4 (left panel) two SEDs computed for PKS 2155–304 with the SSC model described above (the parameters are reported in the figure caption). The scope was to reproduce the lower and higher X-ray states of November 1997, together with the  $\gamma$ -ray data from the discovery observation (Vestrand, Stacy, & Sreekumar 1995) and the brighter  $\gamma$ -ray state of November 1997 (Sreekumar & Vestrand 1997). We (arbitrarily) assumed that the lower and higher X-ray intensity states correspond to the lower and higher  $\gamma$ -ray states, respectively. In order to account for the flaring state, leaving the other parameters unchanged, the break energy of the electron spectrum had to be shifted to higher energies by a factor 1.5. As a consequence, both the synchrotron and IC peaks increase in flux and move to higher energies. However, for the latter the effects are reduced with respect to the “quadratic” relations expected in the Thomson limit, since for these very high energy electrons the suppression due to the Klein-Nishina regime plays an important role.

<sup>1</sup>The Compton emission is computed here with the usual step approximation for the Klein-Nishina cross section, i.e.  $\sigma = \sigma_T$  for  $\gamma\nu_t < mc^2/h$  and  $\sigma = 0$  otherwise, where  $\gamma$  is the Lorentz factor of the electron and  $\nu_t$  is the frequency of the target photon.



The models predict TeV emission at a detectable level. Indeed, towards the completion of this work, we have been informed of the detection of high energy  $\gamma$ -rays by the Mark 6 telescope. In November 1997 the source was seen at its highest flux (Chadwick et al. 1998). The time averaged flux corresponds to  $4.2 \times 10^{-11}$  ph cm $^{-2}$  s $^{-1}$  above 300 GeV (and extending up to  $> 3$  TeV). In fact, the model for the lower intensity state reproduces the TeV emission flux level remarkably well. More observations are needed to study the correlation between the TeV and X-ray fluxes in this source.

## 8 DISCUSSION AND CONCLUSIONS

The X-ray spectra and spectral variability of the three sources discussed above, which are the brightest blue blazars in the X-ray band, appear extremely coherent in the sense that they can be described using analogous spectral laws, where differences between different sources and different states of the same source can be understood as changes in the energy at which the peak power is emitted. Moreover their TeV emission is generally correlated with the X-ray intensity level within the same source.

This behavior can be well understood in the context of the SSC process in a relativistic jet, which seems quite convincingly to account for the SED of blue blazars. In these objects, of relatively low intrinsic power, the synchrotron and IC components tend to peak at the highest energies (X-ray and TeV energies, respectively) and the synchrotron photons dominate the seed radiation field upscattered to  $\gamma$ -ray energies. The models allow us to establish the physical parameters of the jet plasma with relatively little uncertainty and there is general agreement that at least for the three sources discussed above the required values of the Doppler factors are quite high ( $\delta \geq 10$ ), the magnetic fields are  $10^{-1} - 1$  G and the critical electron energy (the break energy in the bpl SSC model) are of order  $10^5$  with values as high as  $10^6$  for Mkn 501 during the 1997 high state.

While the assessment of the radiation mechanisms and physical parameters in the jet seems quite reliable, the inferred variations in the critical electron energies, which seem to correlate well with brightness, potentially contain important clues for an understanding of the variability and of the modes of particle acceleration and injection. Time dependent models for the evolution of the energy distributions of electrons subject to acceleration, injection, propagation and energy losses are required. The problem is in general complex and only some simplified cases have been treated up to now (e.g., Kirk et al. 1998, Dermer et al. 1998, Makino 1998). In addition, light travel time effects through the emitting region may be important (Chiaberge & Ghisellini 1998).

An important point is the measurement and interpretation of lags of the soft photons with respect to the harder ones. These can be due to radiative cooling if the population of injected (accelerated) electrons has a low energy cut off or possibly a sharp low energy break, as clearly shown by Kazanas et al. (1998). If so, the observed lag  $\tau_{obs}$  depends only on the value of the magnetic field (assuming synchrotron losses are dominant, as is roughly the case for these sources) and on  $\delta$ . Their relation can be expressed as

$$B\delta^{1/3} = 300 \left( \frac{1+z}{\nu_1} \right)^{1/3} \left[ \frac{1 - (\nu_1/\nu_0)^{1/2}}{\tau_{obs}} \right]^{2/3} G \quad (1)$$

where  $\nu_1$  and  $\nu_0$  represent the frequencies (in units of  $10^{17}$  Hz) at which the observed lag has been measured.

It is interesting to note that the value of the soft lag inferred for PKS 2155–304 from the *BeppoSAX* observations yields a B and  $\delta$  combination consistent with the parameters obtained *independently* from the spectral fitting, which supports the radiative interpretation of the observed X-ray variability (Tavecchio, Maraschi, & Ghisellini 1998). However the soft *lead* possibly present in the 1998 flare of Mkn 421 should probably be related to the acceleration time scale (Kirk et al. 1998), implying that the time dependence of acceleration/injection events themselves plays a significant role.

In conclusion, the time resolved continuum spectroscopy, made possible by sensitive and broad band instruments like ASCA and *BeppoSAX*, has allowed us to reconstruct the spectra of the emitting high energy electrons in blazars and to follow their evolution in time. Therefore X-ray data of the present quality allow us to probe not only the radiation mechanisms but also the fundamental processes of particle acceleration and transport in relativistic jets.

## 9 REFERENCES

- Aharonian, F., et al. 1997, *A&A*, 327, L5  
Bicknell, G.V., 1994, *ApJ*, 422, 542  
Blandford, R.D., & Rees, M.J., 1978, in Pittsburgh Conf. on BL Lac objects, ed. AM Wolfe, 328  
Catanese, M., et al. 1997, *ApJ*, 487, L143  
Chadwick, P.M., et al., 1998, *ApJ*, in press (astro-ph/9810209)  
Chiaberge, M., & Ghisellini, G., 1998, *MNRAS*, submitted (astro-ph/9810263)  
Chiappetti, L. & Torroni, V. 1997, *IAU Circ.*, 6776, 2  
Chiappetti, L., et al., 1998, submitted  
Dermer, C. D., Sturmer, S. J., & Schlickeiser, R. 1997, *ApJS*, 109, 103  
Dermer, C. D. 1998, *ApJ*, 501, L157  
Edelson, R. A., & Krolik, J. H. 1988, *ApJ*, 333, 646  
Fossati, G., et al., 1997, *MNRAS*, 289, 136  
Fossati, G., et al., 1998, *MNRAS*, 299, 433  
Ghisellini, G., Maraschi, L., Dondi, L., 1996, *A&AS*, 120, 503  
Ghisellini, G. & Maraschi, L., 1996, *ASP Conf. Ser.*, 110, 436  
Ghisellini, G., et al., 1998, *Nucl. Phys. B Proc. Suppl.*, 69, 427  
Giommi, P., et al., 1998a, *Nucl. Phys. B Proc. Suppl.*, 69, 407  
Giommi, P., et al., 1998b, *A&A*, 333, L5  
Kazanas, D., Titarchuk, L. G., & Hua, X.-M. 1998, *ApJ*, 493, 708  
Kirk, J.G., Rieger, F.M., & Mastichiadis, A. 1998, *A&A*, 333, 452  
Lockman, F. J. & Savage, B. D. 1995, *ApJS*, 97, 1  
Mastichiadis, A. & Kirk, J.G., 1997, *A&A*, 320, 19  
Makino, F., 1998, to be published in BL Lac phenomenon  
Maraschi, L., et al., 1994, *ApJ*, 435, L91  
Maraschi, L., 1998, *Nucl. Phys. B Proc. Suppl.*, 69, 389  
Maraschi, L., et al., 1998, to be published in "Tutti i colori degli AGN", third italian conference on AGN, Roma May 18-21, *Memorie SAI*t (astro-ph/9808177)  
Padovani, P., et al., 1998, *Proc. of the Conference "BL Lac Phenomenon"* (Turku, Finland), *PASP Conf. Ser.*, eds. L. Takalo, in press  
Pian, E., et al. 1998, *ApJ*, 492, L17  
Sikora, M. 1994, *ApJS*, 90, 923  
Sreekumar, P. & Vestrand, W. T. 1997, *IAU Circ.*, 6774, 2  
Takahashi, T., et al., 1996, *ApJ*, 470, L89  
Tavecchio, F., Maraschi, L., Ghisellini, G., 1998, *ApJ*, in press (astro-ph/9809051)  
Treves, A., et al., 1998, *Proc. of the Conference "BL Lac Phenomenon"* (Turku, Finland), *PASP Conf. Ser.*, eds. L. Takalo, in press (astro-ph/9811244)  
Ulrich, M.H., Maraschi, L., Urry, C.M., 1997, *Ann. Rev. Astron. and Astroph.*, 35, 445  
Urry, C. M., et al. 1997, *ApJ*, 486, 799  
Vestrand, W. T., Stacy, J. G., & Sreekumar, P. 1995, *ApJ*, 454, L93  
Wehrle, A. E., et al. 1998, *ApJ*, 497, 178  
Wolter, A., et al., 1998, *A&A*, 335, 899